

Magnetotransport and Fermi-surface topology of β'' -(BEDT-TTF)₂AuBr₂: The effects of spin-density-wave formation

M. Doporito, J. Singleton, F. L. Pratt, J. Caulfield, and W. Hayes

Department of Physics, University of Oxford, The Clarendon Laboratory, Parks Road, Oxford OX1 3PU, United Kingdom

J. A. A. J. Perenboom

High Field Magnet Laboratory, University of Nijmegen, Toernooiveld 1, NL-6525 ED Nijmegen, The Netherlands

I. Deckers and G. Pitsi

Laboratorium voor Lage Temperaturen en Hoge-Veldenfysica, Katholieke Universiteit Leuven, Celestijnenlaan 200 D, B-3030 Leuven, Belgium

M. Kurmoo and P. Day

Royal Institution, 21 Albermarle Street, London W1X 4BS, United Kingdom

(Received 10 August 1993)

Magnetoresistance measurements have been made on a number of single-crystal samples of the metallic charge-transfer salt β'' -(BEDT-TTF)₂AuBr₂, using magnetic fields up to 50 T. The experiments have been carried out for a wide range of orientations of the sample with respect to the magnetic field and for temperatures ranging between 80 mK and 4.2 K. The magnetoresistance exhibits a complex series of Shubnikov-de Haas oscillations, an anisotropic angle dependence, and, below 1 K, hysteresis. Both the hysteresis in the magnetoresistance and frequency mixing effects observed in the Shubnikov-de Haas spectrum can be explained by the effects of Shoenberg magnetic interaction, and this mechanism has been successfully used to model the observed Fourier spectrum of the magnetoresistance. The complex Shubnikov-de Haas frequency spectrum of β'' -(BEDT-TTF)₂AuBr₂ is proposed to result from the effects of a spin-density wave on the band structure, which alters the original Fermi surface to produce three two-dimensional carrier pockets. The angle dependence of the Shubnikov-de Haas oscillation amplitudes has been used to deduce the approximate shapes and orientations of these pockets, which are found to be in good qualitative agreement with the proposed model.

I. INTRODUCTION

Charge-transfer salts of the molecule bis(ethylene-dithio)tetrathiafulvalene (BEDT-TTF) form a versatile system for the study of band formation, and as a result have been the focus of intense interest since high-quality crystals became available.¹⁻³ Many different examples of the anion molecule X are possible in the (BEDT-TTF) _{n} X series of salts. This enables variation of the stoichiometry and crystal structure, and hence the band filling and band shape can be adjusted; in this way metallic, semimetallic and semiconducting (BEDT-TTF) salts have been synthesized, some of which may also be superconducting (T_c is typically between 1 and 12 K).¹⁻³

β'' -(BEDT-TTF)₂AuBr₂ has been known since 1986 (Ref. 4) and was one of the first (BEDT-TTF) salts in which Shubnikov-de Haas oscillations (SdHo) due to quasi-two-dimensional carriers were observed.^{5,6} Although band-structure calculations for this material generally yield a Fermi surface consisting of an open section and a single closed hole pocket,^{4,7-9} several different series of Shubnikov-de Haas oscillations were actually observed in the magnetoresistance, corresponding to carrier pockets occupying a small fraction of the Brillouin

zone.⁵ In spite of this interesting behavior, there have been very few subsequent studies of this material,^{6,10,11} possibly because of the very low growth yields of the β'' phase (see Sec. II). In this paper we report studies on a number of high-quality crystals from several growth runs in a variety of magnetotransport experiments. We have found that a number of the apparent SdHo frequencies observed in the magnetoresistance are caused by the Shoenberg magnetic interaction,¹² which generates mixed harmonics of the three true series of oscillations as well as modifying their relative intensity. Angle-dependent magnetoresistance experiments have allowed the areas and shapes of the three closed quasi-two-dimensional pockets which make up the Fermi surface to be deduced; these Fermi-surface pockets may be explained by the existence of a spin-density-wave (SDW) modulation driven by the nesting properties of the open section of the Fermi surface; a wave vector for the SDW of $q = 2\pi(0, 1/nb, 1/2c)$ is found to be consistent with our data, where the interlayer period n is around 2-3 lattice constants.

This paper is organized as follows. Section II provides an introduction to the structure and properties of β'' -(BEDT-TTF)₂AuBr₂, Sec. III describes the procedures followed and Sec. IV summarizes the significant experi-

mental results. An interpretation of the results in terms of spin-density-wave modulation of the band structure is given in Sec. V and the conclusions are listed in Sec. VI.

II. STRUCTURE AND PROPERTIES OF β'' -(BEDT-TTF)₂AuBr₂

β'' -(BEDT-TTF)₂AuBr₂ has the lowest symmetry of all the (BEDT-TTF) charge-transfer salts; it belongs to the triclinic $P\bar{1}$ space group.^{4,7,13} The (BEDT-TTF) molecules form conducting two-dimensional sheets parallel to the ac planes, separated by layers of linear AuBr₂⁻ anions in the b direction;^{4,7,13} the (BEDT-TTF) molecules in the β'' phase stack along the c direction (lattice parameters are given in Table I). The main difference between the β'' phase and other crystal phases possible for (BEDT-TTF) salts is in the direction of the interaction between the (BEDT-TTF) molecules in different stacks. As opposed to the checkered arrangement in the κ phase, for example,^{2,3} the strong intermolecular interactions are at angles of 30° and 60° with respect to the plane of the (BEDT-TTF) molecule.¹⁴ The more complicated interstack interactions lead to β'' -(BEDT-TTF)₂AuBr₂ not being as isotropic in the conducting plane as the κ -phase salts (cf. Refs. 2 and 4). This anisotropy may also be an important factor in the disagreement between transfer integrals based on the room-temperature structure estimated by different groups.^{4,7-9} Unlike the calculations for many other (BEDT-TTF) salts,² there is disagreement between different groups both on the size and the sign of the different components; the only commonly agreed factor is that the largest interaction is along the stacking direction c . The various calculations lead to a Fermi surface with just a single closed pocket or no closed section at all (see Fig. 1). As mentioned above, observations of SdHo in this material indicate the presence of several small carrier pockets;⁵ only the Fermi surface of Mori *et al.*⁴ [Fig. 1(a)] contains a closed section of Fermi surface of a reasonably similar area, although even this is a factor of 2 too large to produce any of the experimental SdHo frequencies.

β'' -(BEDT-TTF)₂AuBr₂ remains metallic down to at least 80 mK (see below), but exhibits several changes in behavior as the temperature is lowered; a decrease in the spin susceptibility begins at around 20 K and is accompanied by a sharp fall in resistance,¹³ whilst electron-spin resonance (ESR) reveals that the g factor of the electrons alters at 6 K.¹³

III. EXPERIMENT

The β'' -(BEDT-TTF)₂AuBr₂ samples were prepared electrochemically.^{4,13} Crystals of the β'' -phase form as

TABLE I. Room-temperature unit-cell parameters of β'' -(BEDT-TTF)₂AuBr₂.

a	b	c
9.027 Å	16.372 Å	5.172 Å
α	β	γ
97.6°	102.94°	92.09°

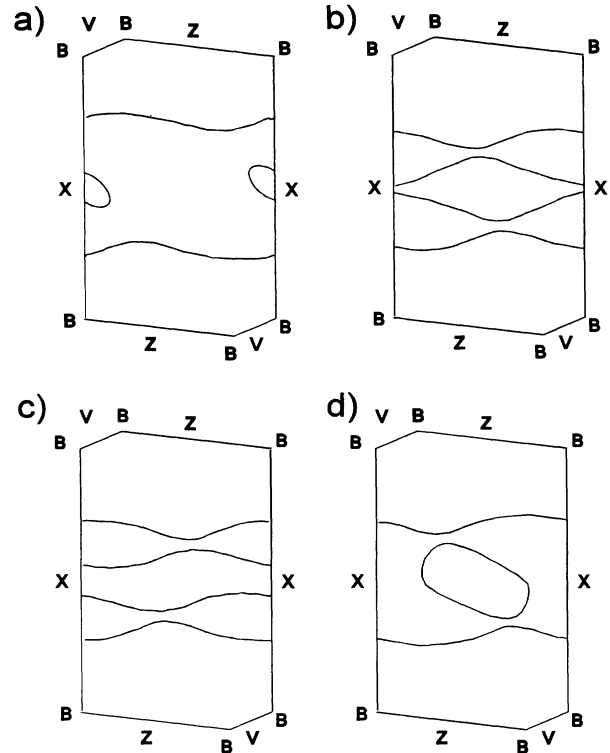


FIG. 1. Section through the first Brillouin zone of β'' -(BEDT-TTF)₂AuBr₂, showing calculated Fermi surfaces according to the following authors; (a) Mori *et al.* (Ref. 4); (b) Kajita *et al.* (Ref. 7); (c) Ducasse (Ref. 8); (d) Green (Ref. 9). The Brillouin zone and all the calculations are based on the room-temperature crystal structure.

distorted hexagonal platelets of typical dimensions $1 \times 0.5 \times 0.1$ mm³. The majority of the (BEDT-TTF)₂AuBr₂ crystals produced are of the semiconducting α or δ phases;^{4,13} a typical batch yields only $\sim 1\%$ of the metallic β'' -phase crystals. Gold wires were attached to both ac platelet faces using platinum paint, giving typical two terminal resistance values of $\sim 50 \Omega$ between the in-plane contacts and $\sim 150 \Omega$ between interplane contacts. Early magnetoresistance studies showed an unusual (negative) magnetoresistance,⁵ probably due to the particular in-plane contact configuration and the relatively large in-plane resistance anisotropy.¹⁵ Since then, it has been found that the interplane magnetoresistance (i.e., with the current applied in the b^* direction, perpendicular to the ac planes) is much less dependent on the contact configuration. In this study all of the magnetoresistance measurements are performed with the current in the interplane b^* direction.

Magnetoresistance measurements were carried out between 80 mK and 4.2 K; low temperatures were provided by dilution refrigerators and ³He and ⁴He cryostats, using calibrated carbon, ruthenium oxide, and germanium resistors as temperature sensors. Some of these cryostats allowed the sample to be rotated *in situ* with a precision of $\pm 0.2^\circ$, and measurements were made for a wide range of orientations of the crystals in the field, involving rotation about the main crystallographic axes. The samples

were initially oriented by measuring the polarized far-infrared reflectivity, which is largest when the radiation is polarized along the stacking direction c ;¹⁶ this normally corresponds to the longer edge of the crystals. A typical crystal shape is sketched in the inset to Fig. 2(d), showing the various in-plane crystal directions which were used as axes for rotating the crystals. The axes are labeled according to the convention of Refs. 4 and 7. Standard low-frequency ac current techniques were used for all measurements except those involving pulsed fields, where either dc or very high frequencies (300 kHz) were employed. To avoid sample heating, the current was generally kept between 0.1 and 100 μA ; care was taken to ensure that the measured resistance values were neither current nor frequency dependent. Steady magnetic fields were provided by a variety of superconductive, resistive, and hybrid magnets at Oxford and Nijmegen, while pulsed fields up to 50 T were provided by the facilities at Leuven.

IV. EXPERIMENTAL MAGNETORESISTANCE DATA

A. General features

Figure 2 shows typical plots of the magnetoresistance of β'' -(BEDT-TTF)₂AuBr₂ crystals as a function of the angle between the magnetic field and the b^* axis (perpendicular to the ac plane) for tilting of the crystal about the a' [Figs. 2(a) and 2(b)] and c [Fig. 2(c)] axes [see the inset to Fig. 2(d) for the relative orientations of these axes]. Several interesting points may be observed. First, the magnetoresistance is around an order of magnitude larger when the field is applied parallel to a' as opposed to parallel to c , presumably due to the anisotropy of the Fermi surface. In addition, when the sample is tilted about the a' axis the low-field magnetoresistance is symmetrical about the normal to the conducting planes and maximum for this direction (see also Refs. 7 and 11). On tilting about the c axis, however, the magnetoresistance is asymmetrical about the origin. This is due to the triclinic structure, where the projection of the b axis on the ac plane is almost parallel to the c direction.^{4,7,13} Similar asymmetrical behavior can be observed in the magnetoresistance of other salts when tilted about an axis which is not parallel to the anion layers.¹⁷ Figure 2(c) also shows that oscillations in the background magnetoresistance are observed at fields above ~ 10 T as a function of tilt angle. These oscillations will be discussed below.

The data in Fig. 2 show that at some angles the magnetoresistance exhibits a maximum at around 10 T, followed by a region of negative slope, whilst at others it shows a point of inflexion at ~ 15 T. This is a general feature of all β'' -(BEDT-TTF)₂AuBr₂ samples studied (see also the data shown in Refs. 5, 10, and 11) and may be contrasted with the monotonically increasing magnetoresistance of many (BEDT-TTF) salts with simple Fermi surfaces [cf. magnetoresistance data, e.g., α -(BEDT-TTF)₂NH₄Hg(NCS)₄ in Ref. 18]; it is indicative of similar sized contributions to the conductivity from more than one type of carrier.¹⁰ Similar behavior is seen in the magnetoresistance of α -(BEDT-TTF)₂KHg(NCS)₄, which also

exhibits a maximum followed by a region of negative slope (see Refs. 19–21 and references therein); however, there is no sign of a strong field-induced phase transition in β'' -(BEDT-TTF)₂AuBr₂ comparable to that seen at ~ 22 T in α -(BEDT-TTF)₂KHg(NCS)₄, even in fields up to ~ 50 T [see Fig. 2(d)]. Other similarities between β'' -(BEDT-TTF)₂AuBr₂ and α -(BEDT-TTF)₂KHg(NCS)₄ will become apparent below.

The magnetoresistance data in Fig. 2 exhibit the presence of more than one frequency of SdHo. On subtracting the slowly varying component of the background magnetoresistance the complexity of the SdHo is revealed; typical data are shown in Fig. 3(a). With the magnetic field applied parallel to b^* , one prominent series of SdHo is observed, apparently modulated by a lower frequency. On tilting about the a' direction to 30° away from b^* , the lower frequency becomes visible as a second set of SdHo. Fourier analysis of the SdHo with the magnetic field applied parallel to b^* [Fig. 3(b)] yields four distinct frequencies at 40, 140, 180, and 220 T together with different harmonic combinations. It is important to identify which of these frequencies correspond to actual carrier pockets, and which are merely artefacts of frequency mixing, or a result of crystal twinning for example. In order to rule out the latter, as well as to check the two dimensionality of the system, the crystal was rotated about several axes in the magnetic field and the angle dependence of the SdH frequencies measured. All were found to follow the $1/\cos\theta$ dependence expected for a quasi-two-dimensional system (here θ is the angle between the magnetic field and b^*) with the same origin for all rotation axes. Twinning can therefore be dismissed as the source of extra SdHo frequencies. In addition, electron paramagnetic resonance data on the same crystal show no sign of the overlapping bands which would result from crystal twinning.¹³

The relative intensities of the different SdHo frequencies as a function of rotation angle about c are compared in the contour plot of Fig. 4(a). This plot is derived from the Fourier transform of the magnetoresistance, with the frequency scale normalized by the $1/\cos\theta$ angular dependence. As mentioned above, the main frequencies are found to be 40, 140, 180, and 220 T. The Fourier amplitudes of the various SdHo frequencies are symmetric for rotation about a' but rather asymmetric for rotation about c , thus mimicking the behavior of the magnetoresistance. In both cases, however, although the 180-T frequency is the strongest for the field perpendicular to the conducting planes, it is the 40- and 200-T frequencies which become dominant as the field is tilted towards the ac plane. An interesting feature occurs when the 180- and the 220-T amplitudes are of similar strength, usually with the field at angles of $\sim 30^\circ$ to b^* ; under these conditions there is a field range in which the SdHo appear to be split [e.g., around $0.10T^{-1}$ in Fig. 3(a)]. These split oscillations are rather similar to those observed in α -(BEDT-TTF)₂KHg(NCS)₄, originally attributed to spin splitting of the Landau levels (see Refs. 20 and references therein).

Tokumoto *et al.*⁶ carried out a de Haas–van Alphen measurement on a sample of β'' -(BEDT-TTF)₂AuBr₂ and

obtained oscillation frequencies which are somewhat higher than those reported in this and other works.^{5,10,11} However, a comparison of the relative strengths of the various frequency components in the data of Tokumoto *et al.*⁶ seems to suggest that the *ac* planes of their sample are not perpendicular to the magnetic field [e.g., the lowest frequency oscillations, corresponding to the 40-T frequency in this work, are very strong compared to the others in the work of Tokumoto *et al.*; cf. Fig. 3(b)]. Tilting of the sample will of course lead to higher oscillation frequencies than expected. The de Haas–van Al-

phen measurements in Ref. 6 were performed using a capacitive technique which involves the suspension of the sample close to an electrode functioning as one plate of the capacitor; we have found that such techniques are prone to misalignment of the sample.

B. Magnetoresistance hysteresis and the Shoenberg magnetic interaction

All of the magnetoresistance data plotted so far have been recorded on the upswing of the magnetic field. On

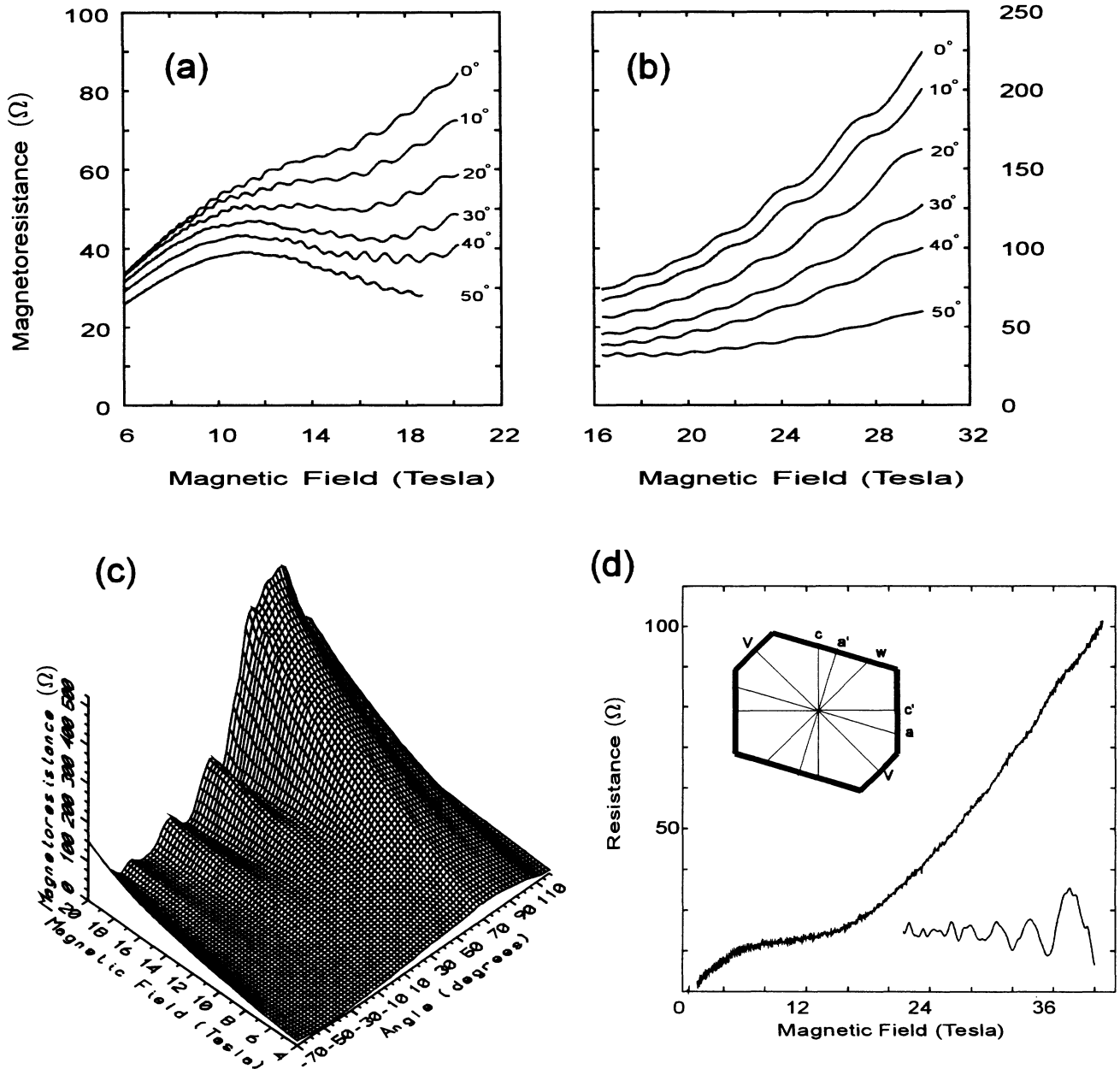


FIG. 2. Magnetoresistance of β'' -(BEDT-TTF)₂AuBr₂ as a function of the angle between the field and the b^* axis (perpendicular to the *ac* plane) for tilting of the crystal about the *a'* [(a) and (b)] and *c* (c) axes. (d) Magnetoresistance recorded using a pulsed magnet; the lower curve shows the SdHo with the slowly varying background subtracted (field parallel to b^*). In all cases the temperature is 500 ± 20 mK, although the electron temperature in (d) is ~ 3 K due to heating from the rapidly changing field. The inset in (d) shows the principal crystal axis in the *ac* plane and typical sample shape.

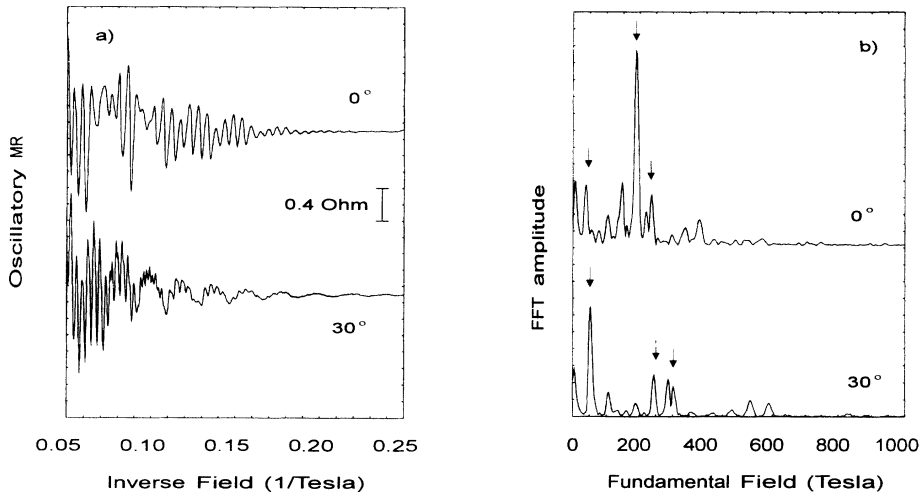


FIG. 3. (a) The oscillatory part of the magnetoresistance of β'' -(BEDT-TTF) $_2$ AuBr $_2$ at 490 mK for magnetic field B parallel to b^* (upper trace, 0°) and for B tilted 30° from b^* about a' towards c (lower trace). (b) The Fourier spectra of the traces shown in (a). Note the primary peaks at 40, 140, 180, and 220 T in the 0° Fourier spectrum plus their harmonics; the peaks at 40, 180, and 220 T are arrowed.

comparing data recorded on upsweeps and downsweeps, shown in Fig. 4(b), it becomes apparent that there is distinct hysteretic behavior below ~ 1 K, an indication of strong internal fields, presumably due to the formation of some sort of magnetic domain structure. Hysteresis between upsweeps and downsweeps of the magnetic field has also been observed in magnetization (de Haas–van Alphen) data by Tokumoto *et al.* at 0.56 K, but not at 2.3 K.⁶

The hysteretic behavior again suggests similarities with α -(BEDT-TTF) $_2$ KHg(NCS) $_4$, which displays a lower magnetoresistance on downsweeps of the magnetic field than it does on upsweeps.^{19–21} In the case of β'' -(BEDT-TTF) $_2$ AuBr $_2$, the hysteresis is exhibited mainly as a shift in the phase and amplitude of the SdHo, rather

than in the background magnetoresistance [cf. Fig. 4(b) of this work and e.g., Fig. 2 of Ref. 21]. The effect of this hysteresis on the SdHo amplitude is shown in the inset to Fig. 4(b), which shows the Fourier amplitude of the 180-T oscillations as a function of temperature for upsweeps and downsweeps. Above ~ 1 K there is no hysteresis and the SdHo amplitudes on the upswep and the downswep are indistinguishable.

There is clearly some form of interaction between two or more pockets of carriers. Indeed we can attempt to explain the observed SdHo in terms of two main pockets with fundamental fields $B_{F1}=40$ T and $B_{F2}=180$ T and combinations such as $B_{F2}\pm B_{F1}$, $2B_{F2}\pm B_{F1}$. A plausible mechanism for such combinations in view of the obvious internal magnetic order, could be via the Shoenberg mag-

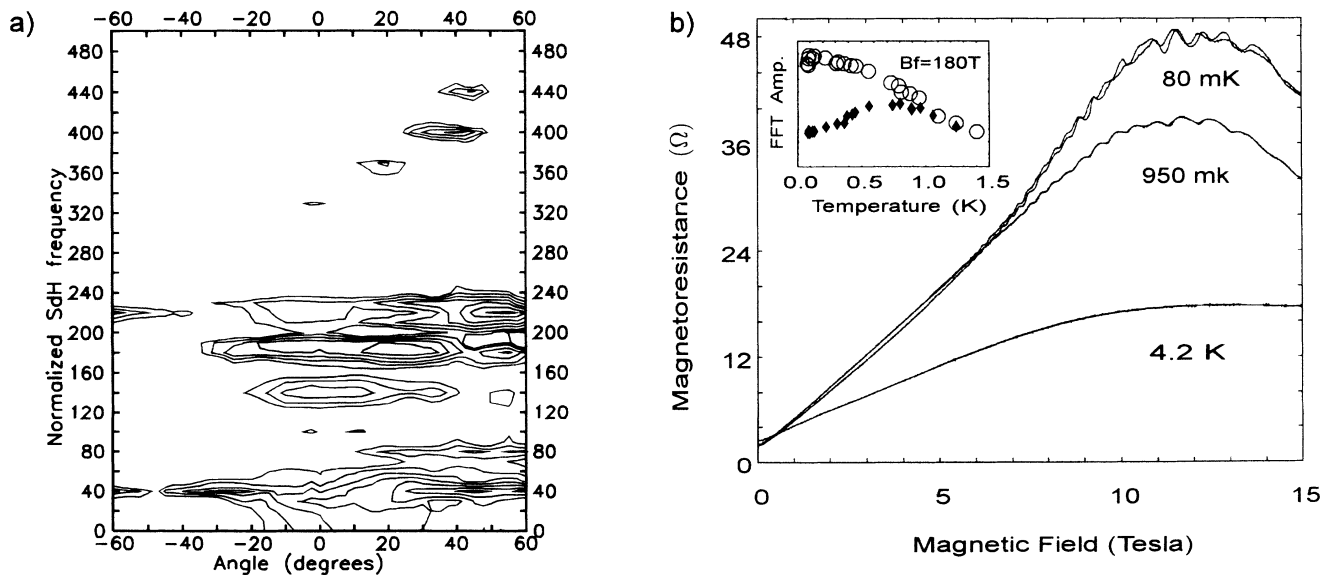


FIG. 4. (a) Contour plot of the frequency spectrum of the magnetoresistance up to 20 T as a function of the tilt angle (θ) about c , normalized by $\cos(\theta)$ to show the two-dimensional angle dependence of the SdH oscillations. (b) The temperature dependence of the magnetoresistance of β'' -(BEDT-TTF) $_2$ AuBr $_2$, which exhibits hysteresis below ~ 1 K (field parallel to b^*). The Fourier amplitude of the 180-T SdHo frequency is shown in the inset, where the circles correspond to upsweeps and the diamonds to downsweeps of the magnetic field.

netic interaction.¹² This would introduce a feedback term due to the fact that the actual field that affects the carriers is $\mathbf{B} = \mu_0(\mathbf{H} + \mathbf{M})$, where \mathbf{H} is the external (applied field and \mathbf{M} is the magnetization containing the oscillatory (de Haas–van Alphen) components. This effect has not previously been reported in organic conductors, probably due to the small magnetization in most materials. In β'' -(BEDT-TTF)₂AuBr₂, however, the hysteresis is indicative of the presence of strong internal fields. Note that Shoenberg magnetic interactions probably also occur in α -(BEDT-TTF)₂KHg(NCS)₄, where similar strong hysteresis is observed.^{19–21}

Simulations using Shoenberg magnetic interactions between the B_{F1} and B_{F2} series are successful in accounting for the sidebands at $180 \text{ T} \pm 40 \text{ T}$ and $360 \text{ T} \pm 40 \text{ T}$, as well as the disappearance of the 180-T series in some of the traces, but cannot reproduce the dominance of the 40- and the 220-T frequencies over the 180-T SdHo at higher angles [see Fig. 4(a)]. At these angles, the strongest second harmonic is that of the 220-T SdHo. All of this would seem to indicate that the 220-T frequency corresponds to a real carrier pocket and is not merely an artefact of mixing. A satisfying fit to the data that includes the Shoenberg magnetic interaction and the presence of three carrier pockets ($B_{F1} = 40 \text{ T}$, $B_{F2} = 180 \text{ T}$, $B_{F3} = 220 \text{ T}$) is shown in Fig. 5.

C. Angle-dependent magnetoresistance oscillations

Having established that the SdHo frequencies $B_{F1} = 40 \text{ T}$, $B_{F2} = 180 \text{ T}$, and $B_{F3} = 220 \text{ T}$ correspond to real, closed sections of Fermi surface, we turn to the angle dependence of their Fourier amplitudes. One of the β'' -

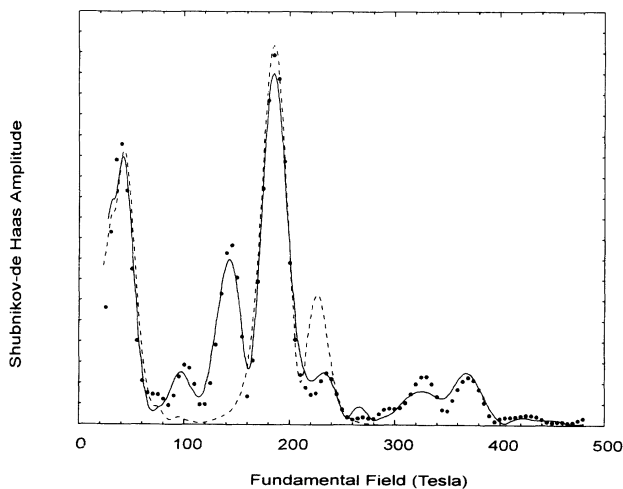


FIG. 5. The Shoenberg magnetic interaction effect. The solid line shows a fit to a Fourier transform of the oscillatory magnetoresistance using the Lifshitz-Kosevich formula with an effective magnetic field $B_{\text{eff}} = \mu_0[H_{\text{ext}} + M(H_{\text{ext}})]$ and the presence of three carrier pockets (B_{F1}, B_{F2}, B_{F3}). The dashed line uses the same parameters but only H_{ext} . The inclusion of the magnetic feedback not only produces new frequencies but also modifies the amplitudes of existing peaks. Experimental data are shown as points (B is parallel to b^* ; the temperature is 490 mK).

(BEDT-TTF)₂AuBr₂ samples was rotated about six different axes, corresponding to the a , c , a' , c' , v , and w directions as defined in the inset to Fig. 2(d), and the magnetoresistance recorded up to 17 T every three degrees; the experiment was carried out at 500 mK. Figure 6 shows the Fourier amplitude of the SdHo due to each pocket as a function of θ , where θ is the angle between the magnetic field and b^* , for rotation about the v and w axes; oscillations are seen in the amplitude which are periodic in $\tan\theta$. Such oscillatory behavior was explained by Yamaji,²² who showed that at certain angles, all the semiclassical k -space closed orbits around a warped cylindrical Fermi surface have approximately the same area. This means that the density of states at the Fermi energy is greatly enhanced, resulting in a maximum in the background magnetoresistance [Fig. 2(c)], and in the amplitude of the SdHo (Fig. 6). The theory was developed by Kartsovnik *et al.*,²³ who considered materials in which the plane of warping can be inclined with respect to the conducting plane. The tilt angles θ at which the maxima occur are given by²³

$$b'k_{\parallel} |\tan\theta| = \pi(i - \frac{1}{4}) \pm A(\phi), \quad (1)$$

where b' is the effective interplane spacing, k_{\parallel} is the radius of the warped cylindrical Fermi surface at a point where the tangent to the surface is perpendicular to the

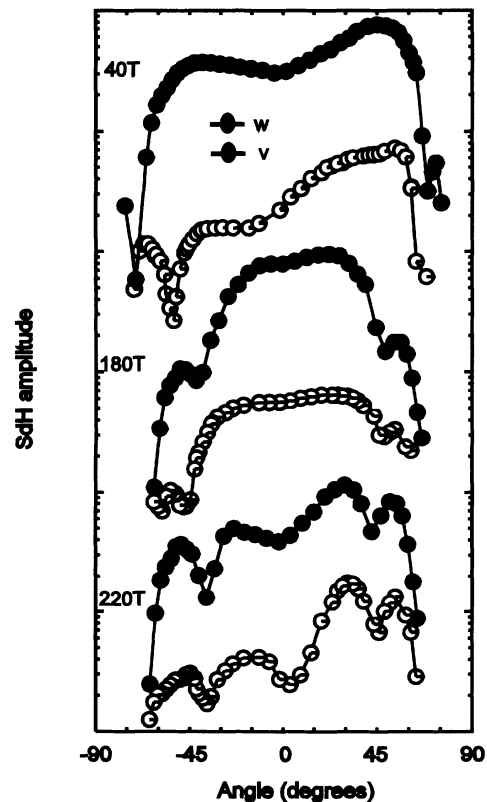


FIG. 6. Angle dependences of the Fourier amplitudes of the three series of SdHo corresponding to real two-dimensional Fermi-surface pockets ($B_{F1} = 40 \text{ T}$, $B_{F2} = 180 \text{ T}$, and $B_{F3} = 220 \text{ T}$) for tilting about the w and v directions. The temperature is 490 mK.

plane of rotation of the magnetic field, i is an integer, and ϕ is the azimuthal angle describing the plane of rotation of the field. The gradient of a plot of $\tan\theta$ against i may thus be used to find one of the dimensions of the Fermi surface, and, if the process is repeated for several planes of rotation of the field, the complete Fermi-surface shape in the conducting plane may be mapped out. $A(\phi)$ is a function of the plane of rotation of the magnetic field, determined by the inclination of the plane of warping with respect to the conducting plane; hence this angle may also be found.²³

Since the magnetoresistance oscillations in β' -(BEDT-TTF)₂AuBr₂ [Fig. 2(c)] result from a combination of three pockets with different shapes and sizes, it is necessary to look at the angle dependence of the amplitude of each individual SdHo series in order to map the Fermi surface. As the SdHo amplitudes become much smaller as $\theta=90^\circ$ is approached, the useful angle range is restricted to about $-70^\circ < \theta < 70^\circ$, which means that only one or two complete oscillations of the tangent term in Eq. (1) (i.e., one or two values of i) are observed. The positions of the 40-, 180-, and 220-T SdHo amplitude maxima are almost symmetrically disposed about the origin for rotation about the a' and a directions, but not symmetrical when the sample is tilted about the c and especially the c' directions. This is in good agreement with the room-temperature crystal structure, where the projection of b , the interplane hopping direction, on the conducting ac plane is almost perpendicular to a .^{4,7,13} Values of $b'k_{\parallel}$ derived from Eq. (1) are shown for the various axes of rotation in Table II. The approximate shapes of the Fermi-surface pockets can be reconstructed from this data; the results of this are shown in Figs. 7(a), 7(b), and 7(c). In addition, since the overall areas of the pockets are known from the SdH frequencies, the periodicity b' in

TABLE II. The product $b'k_{\parallel}/\pi$ calculated from the SdHo amplitude maxima and minima using Eq. (1). The tilt axis directions are defined in Fig. 2.

Tilt axis	40-T pocket	180-T pocket	220-T pocket
c'		0.9 ± 0.2	
a		1.1 ± 0.2	1.3 ± 0.2
a'	0.3 ± 0.1	1.1 ± 0.2	0.8 ± 0.3
c		0.8 ± 0.2	1.4 ± 0.2
v	0.8 ± 0.2	1.4 ± 0.2	1.1 ± 0.2
w	0.3 ± 0.1	1.0 ± 0.2	1.4 ± 0.2

the interplane direction may be estimated; (see Table III). Despite the relatively large errors due to the limited number of oscillations, it is possible to deduce that the Brillouin-zone boundary in the interplane direction at 500 mK is around 2–3 times smaller than the room-temperature value (i.e., $b' \sim 2$ to 3 times the room-temperature crystallographic interplane spacing b ; cf. Tables I and III). Such a superlattice would not, in theory, alter the SdHo frequencies significantly so long as the interplane warping is small; this is in fact the case in most (BEDT-TTF) salts. Possible reasons for such a superlattice will be discussed below.

D. Carrier effective masses

The effective masses of the carriers in β' -(BEDT-TTF)₂AuBr₂ prove to be difficult to evaluate using the conventional application of the Lifshitz-Kosevich (LK) formula^{12,18} to the temperature dependence of the SdHo due to the presence of several interacting frequencies. The hysteresis and frequency mixing alter the amplitudes of the different SdHo components [Fig. 4(b)]. The 40-T

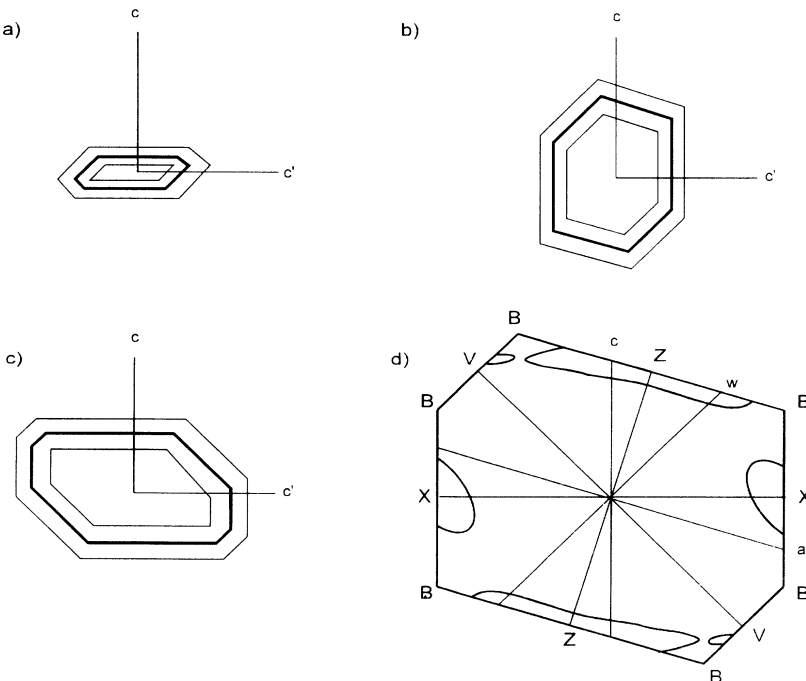


FIG. 7. (a)–(c) Show the shapes and orientations of the three Fermi-surface pockets deduced from the angle dependence of the SdHo amplitudes ($B_{F1}=40$ T, $B_{F2}=180$ T, and $B_{F3}=220$ T). (d) The proposed low-temperature Brillouin zone and Fermi surface resulting from the spin-density-wave reconstruction.

TABLE III. The estimated SdH frequencies calculated using Table II with different multiples of the room-temperature interplane distance $b = 16.372 \text{ \AA}$. These calculations seem to indicate the presence of a $2b$ or $3b$ superlattice.

b'	40-T pocket	180-T pocket	220-T pocket
b	400 T \pm 200 T	1200 T \pm 900 T	1500 T \pm 800 T
$2b$	100 T \pm 60 T	300 T \pm 200 T	400 T \pm 200 T
$3b$	50 T \pm 30 T	130 T \pm 80 T	170 T \pm 80 T
$4b$	30 T \pm 10 T	70 T \pm 40 T	90 T \pm 40 T

frequency poses an additional problem in that the corresponding Fourier amplitude peak is superimposed on the tail of the Fourier amplitude of the background magnetoresistance. Furthermore, the magnetoresistance of β'' -(BEDT-TTF) $_2$ AuBr $_2$ is also highly temperature dependent [Fig. 4(b)], particularly at high fields, and this must be borne in mind when fitting the normalized oscillatory part of the magnetoresistance using the LK formula.^{12,18}

In order to evaluate the effective masses of the carriers corresponding to the 40- and 220-T SdHo frequencies, the crystal was rotated to an angle where the corresponding Fourier amplitudes are large over a reasonable temperature range. When the angle between b^* and the magnetic field is $\sim 30^\circ$, tilting about c towards a' , the 40- and 220-T pocket amplitudes are roughly at local maxima, while the contribution due to the 180-T pocket is still significant. The temperature dependence of the Fourier amplitude of the different SdHo frequencies is shown in Fig. 8. The effect of the internal fields and mixing can be seen in the non-LK behavior of the amplitudes below 1 K, and so fits using the LK formula were only performed above this temperature (fitting over too large a range of temperature probably led to the spread of effective mass

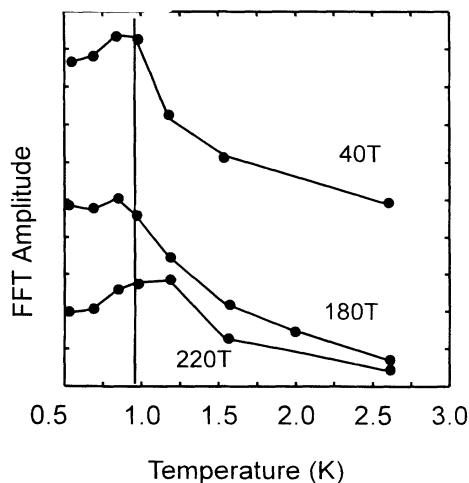


FIG. 8. The temperature dependence of the Fourier amplitudes of the three series of SdHo ($B_{F1} = 40 \text{ T}$, $B_{F2} = 180 \text{ T}$, and $B_{F3} = 220 \text{ T}$). The vertical line shows the low-temperature limit of the fits to the Lifshitz-Kosevich formula. The magnetic field is applied at 30° to b^* (see text).

values in early papers, e.g., Refs. 5 and 10). Effective masses of $2.6 \pm 0.2 m_e$, $2.0 \pm 0.2 m_e$, and $3.5 \pm 0.3 m_e$ (corrected to 0°) were obtained for the Fermi-surface pockets corresponding to the 40-, 180-, and 220-T SdHo frequencies, respectively.

V. DISCUSSION

The calculated Fermi surface that corresponds most closely to that deduced from the SdHo data is that due to Mori *et al.*; it has just one closed hole pocket of $\sim 5\%$ of the room-temperature Brillouin-zone area centered on the X point, together with a pair of open sections⁴ [see Fig. 1(a)]. Although the calculated closed hole pocket is a factor of 2–5 too large to correspond to any of the observed SdHo frequencies, it should be remembered that the pocket is close to the top of the hole band, so that very small adjustments of the intermolecular overlaps could result in a large reduction in pocket area. However, the calculated Fermi surface contains no obvious candidate for the remaining closed pockets observed in the experiments reported here. In view of the evidence for a low-temperature magnetic ground state of β'' -(BEDT-TTF) $_2$ AuBr $_2$, seen in the spin susceptibility below $\sim 20 \text{ K}$ (Ref. 13) and the presence of hysteresis in the magnetoresistance below $\sim 1 \text{ K}$, we propose that the additional SdHo frequencies are the result of closed pockets produced by a spin-density-wave (SDW) modulation. This SDW would be expected to be driven by the good nesting properties of the quasi-one-dimensional (quasi-1D) part of the Fermi surface for an in-plane wave-vector component of $2\pi/2c$. The result of such a SDW modulation on the calculated Fermi surface is shown in Fig. 7(d); a small pocket (holelike) is produced close to V , together with a larger anisotropic closed section of the Fermi surface (electronlike). The band filling is such that there should be equal numbers of electrons and holes, so that the total area of the two-hole pockets should be the same as the area of the electron pocket. In this way, if we identify the two-hole pockets with SdHo frequencies B_{F1} and B_{F2} , the SdHo due to the electron pocket should occur at the sum of these frequencies, namely $B_{F3} = 220 \text{ T}$. A comparison of Figs. 7(d) and 7(a)–7(c) shows that there is reasonable qualitative agreement between this proposed SDW ground state and the experimental Fermi-surface shapes and orientations calculated from the angle dependence of the SdHo amplitudes.

Although quasi-1D materials such as the TMTSF (tetramethyltetraselenafulvalene) charge-transfer salts are well known to be prone to SDW formation,^{2,3} little attention has been paid to the possibility of SDW's existing in (BEDT-TTF) salts, in spite of the good nesting characteristics of the open sections of Fermi surface which are often present. The reason for this is that the effects of SDW are more subtle than in materials with only a quasi-1D Fermi surface, due to the additional presence of the two-dimensional carriers; the two-dimensional carriers can “short-circuit” major reconstructions taking place in the quasi-1D sections of the Fermi surface, making the experimental signature of the SDW much weaker to detect. However, the existence of SDW order has been

recently proposed^{17,19–21} to explain the field-induced resistive “kink” transitions observed around ~ 20 – 35 T in the α -(BEDT-TTF)₂MHg(NCS)₄ ($M = \text{Tl, K, Rb}$) family of salts. Although the resultant low-temperature band structure is still the subject of speculation, the overwhelming body of experimental evidence favors the existence of SDW at low temperatures in these materials. The SDW leads to antiferromagnetic behavior in the α -(BEDT-TTF)₂MHg(NCS)₄ salts,¹⁹ plus hysteresis in the magnetoresistance^{19–21} and the presence of extra SdHo frequencies.^{17,21} All of these features are also observed in β' -(BEDT-TTF)₂AuBr₂ in the experiments described in this work, suggesting a similar reason for this material’s low-temperature behavior.

In Sec. IV C we showed that the repeat period for the electronic structure in the interplane direction b' , as deduced from the angle-dependent oscillations in the SdHo amplitudes, was a factor 2–3 larger than the crystallographic interplane distance b measured at room temperature. This suggests that there is some interplane component in the SDW ordering; magnetic ordering with an interplane component has been suggested as a factor in the observation of the field-induced resistive kink transitions in the α -(BEDT-TTF)₂MHg(NCS)₄ ($M = \text{Tl, K, Rb}$) salts.²¹

Finally, it will be noted that the effective masses of the carriers in β' -(BEDT-TTF)₂AuBr₂ are a factor ~ 3 larger than the values obtained in the band-structure calculations.^{4,7–9} Similar behavior is observed in a number of (BEDT-TTF) salts;²⁴ band-structure calculations in (BEDT-TTF) salts can generally reproduce the experimentally observed Fermi-surface shapes reasonably well, but overestimate the bandwidth (i.e., underestimate the effective mass).²⁴ Recent cyclotron resonance measurements²⁵ demonstrate that it is primarily the electron-electron interactions in (BEDT-TTF) salts which lead to the enhancement of the effective mass measured in SdHo experiments over the theoretical band-structure mass. Using the Brinkman and Rice mass enhancement formula derived from the Gutzwiller approximation to the Hubbard model, we have previously shown that the renormalization of the effective mass in α -(BEDT-TTF)₂MHg(NCS)₄ ($M = \text{K, NH}_4$) and κ -(BEDT-TTF)₂Cu(NCS)₂ is of approximately the expected size.²⁵ Similar considerations apply to the Pauli spin splitting in these materials, and the most recent data indicate that the g factor of the 2D carriers is probably also renormalized by electron-electron interactions.¹⁸

VI. CONCLUSION

We have performed a variety of magnetoresistance measurements on a number of single crystals of β' -(BEDT-TTF)₂AuBr₂. The magnetoresistance anisotropy

and complex Shubnikov–de Haas frequency spectrum of this material can be understood in terms of the effect of a spin-density wave on the band structure, which alters the original Fermi surface to produce three two-dimensional carrier pockets corresponding to the measured Shubnikov–de Haas oscillation frequencies of $B_{F1} = 40$ T, $B_{F2} = 180$ T, and $B_{F3} = 220$ T. The angle dependence of the Shubnikov–de Haas oscillations has been used to deduce the approximate shapes and orientations of these pockets, and the results are in qualitative agreement with the model proposed.

Evidence for the spin-density wave is also given by the transitions in behavior which β' -(BEDT-TTF)₂AuBr₂ undergoes on cooling; the resistance decreases suddenly at ~ 20 K, ESR measurements show a magnetic transition around 6 K, and below ~ 1 K there is significant hysteresis in the magnetoresistance. These magnetic transitions are likely to be driven by the nesting properties of the open section of the Fermi surface. The hysteresis in the magnetoresistance suggests that the Shoenberg magnetic interaction is responsible for producing additional combination frequencies seen in the Shubnikov–de Haas oscillations, and this mechanism has been used to model the observed Fourier spectrum of the magnetoresistance successfully.

Note added in proof. Ducasse (private communication) has recalculated the electronic band structure within the extended Hückel model but using the double ξ basis set [see M. H. Whangbo *et al.*, *J. Amer. Chem. Soc.* **107**, 5815 (1985)]. The intrastack interactions are quite sensitive to the nature of the atomic orbitals leading to the overlaps. Consequently, the Fermi surface may be transformed from 1D to 2D. The Fermi surface calculated using the simple ξ set is thus composed of two 1D sections [Fig. 1(c)], while for the double ξ set one of the 1D sections is closed into one 2D pocket of $\sim 7\%$ of the Brillouin zone. This resembles closely the Fermi surface calculated by Mori *et al.* [Fig. 1(a)].

ACKNOWLEDGMENTS

This work was supported by the Science and Engineering Research Council (UK). The Nijmegen High Field Magnet Laboratory is supported by Stichting voor Fundamenteel Onderzoek der Materie (FOM) and by the European Community Large Installations Plan. The pulsed field work at Leuven was carried out by J.C. under the ERASMUS scheme. We should like to thank Dennis Rawlings, Hung van Luong, and Jos Rook for their expert technical assistance, Stephen Hill for the dilution refrigerator measurements, and Klaas van Hulst for his encouragement and help. We are also grateful to Laurent Ducasse and Mark Green for allowing us access to their band-structure calculations in advance of publication (Refs. 8 and 9).

¹For a recent review, see, *Proceedings of the International Conference on Science and Technology of Synthetic Metals, Göteborg, Sweden, 1992* [Synth. Met., **56-8**, XX (1993)].

²T. Ishiguro and K. Yamaji, *Organic Superconductors*

(Springer-Verlag, Berlin, 1990).

³*Organic Superconductivity*, edited by V. Z. Kresin and W. A. Little (Plenum, New York, 1990).

⁴T. Mori, F. Sakai, G. Saitoh, and H. Inokuchi, *Chem. Lett.*

- 1986, 1037 (1986).
- ⁵F. L. Pratt, A. J. Fisher, W. Hayes, J. Singleton, S. J. R. M. Spermon, M. Kurmoo, and P. Day, *Phys. Rev. Lett.* **61**, 2721 (1988).
- ⁶M. Tokumoto, N. Kinoshita, Y. Tanaka, K. Murata, and H. Anzai, *Jpn. J. Appl. Phys.* **7**, 395 (1992); M. Tokumoto, A. G. Swanson, J. S. Brooks, C. C. Agosta, S. T. Hannahs, N. Kinoshita, H. Anzai, M. Tamura, H. Tajima, H. Kuroda, and J. R. Anderson, Ref. 3, p. 191; M. Tokumoto, A. G. Swanson, J. S. Brooks, C. C. Agosta, S. T. Hannahs, N. Kinoshita, H. Anzai, M. Tamura, H. Tajima, H. Kuroda, A. Ugawa, and K. Yakushi, *Physica B* **184**, 508 (1993).
- ⁷K. Kajita, Y. Nishio, S. Moriyama, W. Sasaki, K. Koto, H. Kobayashi, and A. Kobayashi, *Solid State Commun.* **60**, 811 (1986).
- ⁸L. Ducasse (unpublished).
- ⁹M. A. Green (unpublished).
- ¹⁰M. Doporto, F. L. Pratt, W. Hayes, J. Singleton, T. Janssen, M. Kurmoo, and P. Day, *Synth. Met.* **41-43**, 1903 (1991).
- ¹¹F. L. Pratt, M. Doporto, J. Singleton, T. J. B. M. Janssen, J. A. A. J. Perenboom, M. Kurmoo, W. Hayes, and P. Day, *Physica B* **177**, 333 (1992).
- ¹²D. Shoenberg, *Magnetic Oscillations in Metals* (Cambridge University Press, Cambridge, 1984).
- ¹³M. Kurmoo, D. R. Talham, P. Day, I. D. Parker, R. H. Friend, A. M. Stringer, and J. A. K. Howard, *Solid State Commun.* **61**, 459 (1987); M. Kurmoo (unpublished).
- ¹⁴Two other β'' -phase salts, β'' -(BEDT-TTF)₂ AuI₂Br and β'' -(BEDT-TTF)₂ICl₂, have been prepared; see A. Ugawa, Y. Okawa, K. Yakushi, H. Kuroda, A. Kawamoto, J. Tanaka, M. Tanaka, Y. Nogami, S. Kagoshima, K. Murata, and T. Ishiguro, *Synth. Met.* **29**, 1988; K. Kajita *et al.*, Ref. 7.
- ¹⁵W. Kang and D. Jerome (private communication); H. C. Montgomery, *J. Appl. Phys.* **42**, 2071 (1971); B. F. Logan, S. O. Rice, and R. F. Wick, *J. Appl. Phys.* **42**, 3075 (1971).
- ¹⁶F. L. Pratt, W. Hayes, A. J. Fisher, J. Singleton, S. J. R. M. Spermon, M. Kurmoo, and P. Day, *Synth. Met.* **29**, F667 (1989); H. Kuroda, K. Yakushi, H. Tajima, A. Ugawa, M. Tamura, Y. Okawa, A. Kobayashi, R. Kato, H. Kobayashi, and G. Saito, *Synth. Met.* **27**, A491 (1988).
- ¹⁷M. V. Kartsovnik, A. E. Kovalev, and N. D. Kushch, *J. Phys. I (France)* **3**, 1187 (1993).
- ¹⁸J. Singleton, F. L. Pratt, M. Doporto, J. Caulfield, W. Hayes, I. Deckers, G. Pitsi, F. Herlach, T. J. B. M. Janssen, J. A. A. J. Perenboom, M. Kurmoo, and P. Day, *Synth. Met.* **55-57**, 2198 (1993).
- ¹⁹T. Sasaki and N. Toyota, *Solid State Commun.* **82**, 447 (1992); T. Sasaki, H. Sato, and N. Toyota, *Synth. Met.* **42**, 2211 (1991).
- ²⁰J. S. Brooks, C. C. Agosta, S. J. Klepper, M. Tokumoto, N. Kinoshita, H. Anzai, S. Uji, H. Aoki, A. S. Perel, G. J. Athas, and D. A. Howe, *Phys. Rev. Lett.* **69**, 156 (1992); T. Osada, R. Yagi, S. Kagoshima, N. Miura, M. Oshima, and G. Saito, *Phys. Rev. B* **41**, 5428 (1990).
- ²¹F. L. Pratt, J. Singleton, M. Doporto, A. J. Fisher, T. J. B. M. Janssen, J. A. A. J. Perenboom, M. Kurmoo, W. Hayes, and P. Day, *Phys. Rev. B* **45**, 13 904 (1992).
- ²²K. Yamaji, *J. Phys. Soc. Jpn.* **58**, 1520 (1989).
- ²³M. V. Kartsovnik, V. N. Laukhin, S. I. Pesotskii, I. F. Schegolev, and V. M. Yakovenko, *J. Phys. I (France)* **2**, 89 (1992).
- ²⁴N. Toyota, E. W. Fenton, T. Sasaki, and M. Tachiki, *Solid State Commun.* **72**, 859 (1989); F. L. Pratt, J. Singleton, M. Kurmoo, S. J. R. M. Spermon, W. Hayes, and P. Day, in *The Physics and Chemistry of Organic Superconductors*, edited by G. Saito and S. Kagoshima, Springer Proceedings in Physics, Vol. 51 (Springer-Verlag, Berlin, 1990), p. 200.
- ²⁵S. Hill, J. Singleton, F. L. Pratt, M. Doporto, W. Hayes, T. J. B. M. Janssen, J. A. A. J. Perenboom, M. Kurmoo, and P. Day, *Synth. Met.* **56**, 2566 (1993); J. Singleton, F. L. Pratt, M. Doporto, W. Hayes, T. J. B. M. Janssen, J. A. A. J. Perenboom, M. Kurmoo, and P. Day, *Phys. Rev. Lett.* **68**, 2500 (1992).